

Scientific Paper

Doi: <http://dx.doi.org/10.1590/1809-4430-Eng.Agric.v44e20230168/2024>

STUDY OF THE THERMAL ENVIRONMENT AND MARGINAL EFFECTS OF A SUNKEN SOLAR GREENHOUSE

Weiwei Cheng¹, Changchao Wang², Yu Wang², Mengjun Chen²,
Penghui Qiao², Zhonghua Liu^{1*}

^{1*}Corresponding author. Shanxi Agricultural University, College of Urban and Rural construction/Taigu, China.

E-mail: lzh6175305@163.com | ORCID ID: <https://orcid.org/0009-0001-5308-9606>

KEYWORDS

microclimate,
mathematical
modelling, theoretical
modelling, thermal
comfort,
environmental quality.

ABSTRACT

A sunken solar greenhouse is a unique structure used in China that has good thermal performance and a low cost. To explore the thermal environment and the marginal effect area under the trellis membrane in a sunken solar greenhouse, daytime heat absorption and nighttime exothermic models of the greenhouse were established based on existing theories and hypotheses. An experimental study of the three-dimensional thermal environment of a solar greenhouse was also conducted in the Jinzhong Basin of Shanxi Province. The daytime heat absorption model described how the internal thermal environment of the greenhouse changes in three dimensions, while the nighttime model calculated the amount of heat released at night. The results showed that the rate of change in the maximum temperature difference along the height direction in the greenhouse was 13 times that along the vertical direction, and three times that along the horizontal direction. We also observed that the marginal effect area under the membrane varied over time and by month. The minimum value of the marginal effect area occurred at the middle cross-section, spanning the middle position of the greenhouse, and the maximum height was 2.7 m. The results of this study can provide theoretical guidance and experimental data for the thermal environment of greenhouses of the same type in the Jinzhong Basin of Shanxi Province, thus providing a basis for environmental regulation and low-temperature margins in greenhouses.

INTRODUCTION

A sunken solar greenhouse was the original type of greenhouse used in China; its soil wall has been found to offer better thermal storage performance than reinforced concrete materials, and it is cheaper and better insulated than typical greenhouses (Zhang et al., 2010). A sunken heliostat is used to improve the indoor temperature and to create a suitable environment for plant growth. According to the theory of heat transfer, the main indicators for evaluating the thermal environment of a solar greenhouse are the surface temperature and heat storage of the enclosure structure, the soil temperature, and the indoor environmental temperature (Guan et al., 2012). Indoor air temperature is the most synergistic plant body temperature, and is the factor to which the healthy growth of plants is most sensitive (Yu et al., 2015). Indoor air temperature also varies with the same trends as the outdoor air temperature, the indoor

ground temperature, the surface temperature of the wall and the surface temperature of the wall outer covering (Zhang et al., 2019; Huang et al., 2013; Hu et al., 2014). A study of the three-dimensional thermal environment of a sunken solar greenhouse can therefore provide a basis for determining plant growth and development, wall insulation and soil heat transfer. Research on the thermal environment of solar greenhouses is mainly concentrated in China, and the main research directions involve indoor environmental models (Zhang et al., 2018; Xu et al., 2019), indoor soil heat transfer models (Zhang et al., 2012), heat transfer models, materials, and types of indoor walls (Tong & Christopher, 2019; Ma et al., 2019; Bao et al., 2019). Most foreign greenhouses are large, continuous structures, and relatively little research has been conducted on the microclimate of solar greenhouses (Ahamed et al., 2018). Solar greenhouse temperatures

¹ Shanxi Agricultural University, College of Urban and Rural construction/Taigu, China

² Shanxi Agricultural University, College of Agricultural Engineering/Taigu, China

Area Editor: Gizele Ingrid Gadotti

Received in: 11-29-2023

Accepted in: 3-4-2024

vary significantly on a daily basis, and are unevenly distributed in space and time (Tong et al., 2019). Previous studies have analysed indoor temperatures with data captured at a single monitoring point (or only a few points); this approach has certain limitations, and tends to overlook global extreme temperature points (Zhang et al., 2021). In this paper, we establish theoretical formulas and experimental methods to investigate the thermal environment effects of sunken heliostats, in order to provide theoretical and experimental data as a basis for the improvement of sunken heliostat arch structures and heating.

Theoretical modelling and experiments

Theoretical modelling

Daytime heat-absorption model

In previous models (Han et al., 2014; Xu et al., 2019; Ma et al., 2013), the total amount of solar

scattering has been calculated by using the visible angle of the space point to calculate the amount of scattered radiation absorbed by an indoor point, which is limited to the cross section. However, scattered radiation is isotropic, and none of the above models considers the relationship between the amount of solar radiation absorbed by an indoor spatial point and its coordinate value. Based on the assumption of anisotropic uniformity of scattered light, the amount of solar scattered radiation absorbed by the interior space point Q is considered to be equal to the total amount of solar scattered radiation inside the solar greenhouse multiplied by the volume coefficient, and the volume coefficient is the ratio between the point Q with the southern shed film boundary point of the solar greenhouse to form a curved body and the volume of the whole solar greenhouse, as shown in Figure 1. The amount of scattered radiation received at the point Q in the sunken solar greenhouse is related to the ratio $V_{Q-ACGE}:V_{ACDB-EFHG}$.

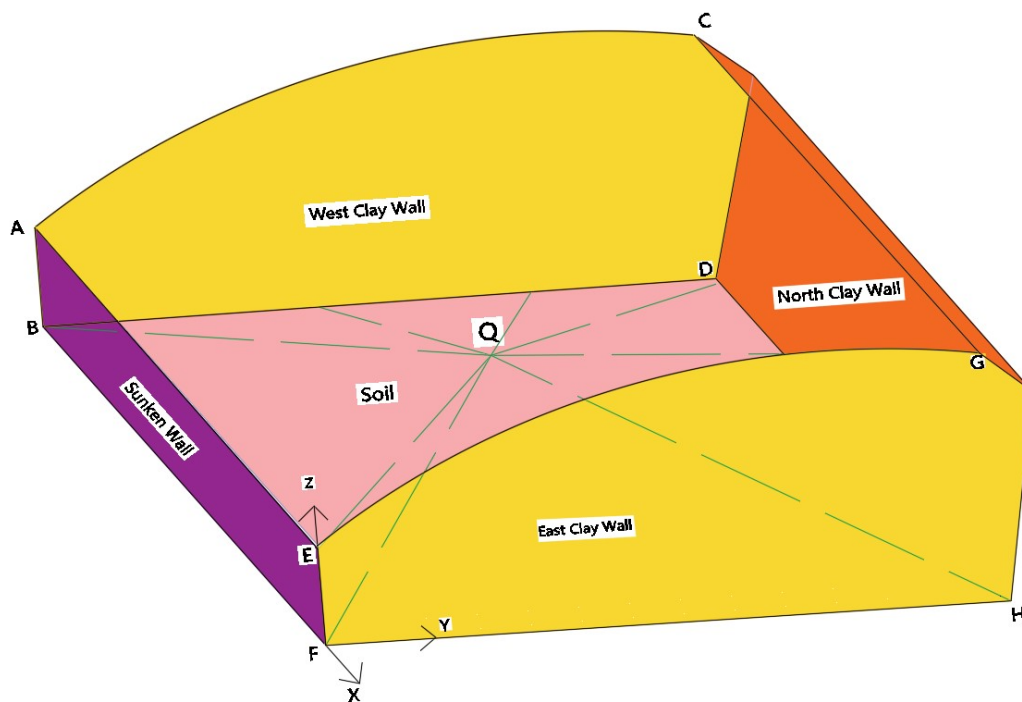


FIGURE 1. Diagram showing the scattered radiation in a sunken solar greenhouse.

TABLE 1. Nomenclature used in this study.

Parameter	
S_{QZ}	Amount of direct solar radiation received at a spatial point Q (W/m^2)
Q_S	Amount of solar scattered radiation received at a spatial point Q inside the greenhouse (W/m^2)
S'_1	Direct solar illumination passing through the atmosphere to the outer surface of the greenhouse membrane (W/m^2)
S_{Qs}	Solar scattered radiation illuminance passing through the atmosphere to the outer surface of the greenhouse membrane (W/m^2)
θ	Angle of incidence of daylight

T_1	Direct light transmission rate of the film at different roof angles (%)
T_2	Scattered light transmittance of the film at different roof angles (%)
T_{z0}	Transmittance of a dry, clean, new covering material to direct light radiation at an incidence angle of 0°
γ_1	Loss of shading of the greenhouse structural materials
γ_2	Loss of light transmission of the covering material due to deterioration
γ_3	Loss of light transmission due to dust contamination and droplets of condensation
H_{aze}	Haze of the covering material (%).
η	Influence coefficient of point scattering
$(\int zdx + \iint 1/2dydz) \times L$	Volume of the greenhouse (m^3)
x, y, z	Coordinate values of point Q (m)
b	Length of the upper bottom of the northern soil trapezoidal wall (m)
D	Sunken depth of the greenhouse (m)
W, L, H	Span, length and ridge height of the sunken solar greenhouse (m)
A_s	Floor area of the greenhouse (m^2)
q	Heat per unit area (w/m^2)
α	Heated area correction factor
q	Reflectance of indoor sunlight

The amount of indoor space point direct solar radiation is calculated with reference to the direct light transmittance of solar greenhouse, as proposed by Xu et al. (2019), with respect to the angle of incidence. The absorbed direct solar energy inside the solar greenhouse is

$$S_{Qz} = S'_1 \times T_1 \times (1 - H_{aze}) \quad (1)$$

According to a study of the solar scattering principle by Ma et al. (2013), the amount of scattering for a sunken solar greenhouse consists of two parts: the conversion of direct solar partial light through the plastic trellis film into indoor scattering, and the outdoor solar scattering light through the plastic trellis film becomes indoor greenhouse scattering amount directly. According to the above conclusions and assumptions, the amount of

solar scattered radiation absorbed by indoor space points can be obtained as

$$S_{Qs} = (H_{aze} \times S'_1 \times T_1 + S'_2 \times T_2) \times (1 - \eta) \quad (2)$$

$$\eta = \frac{(D - H)Ly/3 - WLz/3 - (3LHW + bHL)/6}{(\int zdx + \iint 1/2dydz) \times L}$$

The heat absorbed in the interior of the greenhouse is related to the solar radiation as (Ma CW, Zhao SM, Cheng JY, et al.) $q = Q/A_s = \alpha\tau S(1 - \rho)$.

According to eqs (1) and (2), and taking into account the reflectance of the sun at the spatial point in the greenhouse, the heat per unit area absorbed at the

spatial point in the solar greenhouse during the daytime is as follows:

$$q = \alpha S = \alpha(S_{Qz} + S_{Qs}) = \alpha S'_1 T_1 (1 - \eta H_{aze}) + \alpha S'_2 T_2 (1 - \eta) \quad (3)$$

To calculate the direct solar radiation and scattering, we use the empirical model proposed by Liu & Jordan (1960), in which solar scattering radiation determined according to a certain proportion of direct

solar radiation under clear and cloudless weather, as shown in eqs (4) and (5):

$$T_s = 0.2710 - 0.2939 T_z \quad (4)$$

$$S'_1 = S_0 T_z \quad S'_2 = S_0 T_s \quad (5)$$

Equation (3) can be simplified to give

$$q = \{ [(1 - \eta \cdot H_{aze}) T_1 - 0.2939 (1 - \eta) T_2] T_z + 0.2710 (1 - \eta) \cdot T_2 \} \alpha S_0 \quad (6)$$

From [eq. (3)], we know that: (i) the radiation heat received by a point inside the sunken solar greenhouse is related to η ; (ii) the value of η is affected by the y and z coordinates of the point, but has very little relationship to the vertical x coordinate; (iii) when z is constant, η gradually decreases with an increase in y , and the closer to the north wall, the higher the temperature; (iv) when y is constant, it gradually decreases with an increase in z , and the heat absorbed by the space point increases (that is, when heat loss is not considered, the closer to the shed film); (v) when x is constant, the changes in the values of y and z are equal, and the ratio of the change in z along the vertical direction and y along the horizontal direction is $W/(H-D)$, where W is the span of the greenhouse (8–12) m, and $H-D$ refers to the ridge height minus the sunken depth, [5–(1.2–2)] m. Hence, the ratio of $W/(H-D)$ is greater than two, which shows that the rate of change in the greenhouse temperature along the vertical direction is greater than along the lateral direction.

Nighttime heat-dissipation model

Based on studies of the thermal environment of each component of the solar greenhouse carried out by Hu & Fan (2018), Zhang (2012) and Huang et al. (2013), the following assumptions were made about the nighttime thermal environment changes in each component of the sunken solar greenhouse:

- (i) The indoor and outdoor temperatures decrease linearly but unequally over time, and the rates of temperature decrease at each point in the indoor space are equal;
- (ii) The temperature of the outer surface of the earthen walls on the east, west and north sides of the interior undergoes a linear decrease over time;
- (iii) The temperature of the upper surface of the indoor soil decreases linearly with time, and the heat generated by indoor plant respiration is neglected.

At night, the air in the greenhouse and the outdoor heat transfer by conduction, the formula for heat transfer by conduction between the interior of the heliostat and the outdoor is (Ntinias, 2015)

$$Q = \mu_j A_j (t_1 - t_2) \quad (7)$$

TABLE 2. Parameter notation.

Parameter	
Q	Conduction heat loss (W)
μ_j	Heat transfer coefficient of the maintenance structure ($W/m^2 \cdot K$)
A_j	Area of the enclosed structure (m^2)
t_1	Temperature of the inner side of the plastic film of the solar greenhouse (K)
t_2	Outdoor temperature (K)
Φ	Heat flow (W)
μ	Convective heat transfer coefficient ($W/m^2 \cdot K$)
A	Area of the greenhouse floor (m^2)

T_g	Ground temperature or back wall surface temperature (K)
T_f	Ground air temperature or back wall air temperature (K)
ΔQ_a	Indoor nighttime heat loss (W)
ΔQ_s	Nighttime heat release from soil (W)
ΔQ_w	Nocturnal heat release from walls (W)
ΔQ_c	Crop heat release at night (W)
ΔQ_{Ia-Oa}	Nighttime heat exchange between indoor and outdoor gases (W)
A_{si}	Soil area of the greenhouse (m ²)
$\frac{dT_{si}}{dt}$	Rate of change in the temperature of the lower surface of the soil in the greenhouse with time, constant value (K/s)
$\frac{dT_g}{dt}$	Rate of change in the air temperature at the upper surface of the soil interior with time, constant value (K/s)
A_{wn} , A_{we} , A_{ww}	Areas of the walls on the north, east and west sides of the greenhouse, respectively (m ²)
$\frac{dT_{wn}}{dt}$, $\frac{dT_{we}}{dt}$, $\frac{dT_{ww}}{dt}$	Surface temperatures of the walls on the north, east and west sides of the greenhouse velocity of change with time (K/s)
$\frac{dT_{gn}}{dt}$, $\frac{dT_{ge}}{dt}$, $\frac{dT_{gw}}{dt}$	Rate of change of surface temperatures of the walls on the north, east and west sides of the greenhouse with time (K/s)
$\frac{dT_{out}}{dt}$	Rate of change of outdoor gas temperature with time, as a constant value (K/s)

From thermodynamics, the heat transfer phenomenon generated by the flow of fluid at a solid surface is called convective heat exchange. Convective heat exchange is generated between the air in the greenhouse and the ground at night, and the formula for this heat exchange is:

$$\Phi = \mu A (T_g - T_f) \quad (8)$$

The heat loss from the indoor air is equal to the heat released from the indoor soil, the heat released from

the indoor walls, the heat released from plant respiration, the leakage from the greenhouse seams and the heat loss from indoor-outdoor air exchange at the south membrane. We therefore have:

$$\Delta Q_a = \Delta Q_s + \Delta Q_w + \Delta Q_c - \Delta Q_{Ia-Oa} \quad (9)$$

Based on the assumptions set out in Section 2.1.2, the heat balance equation for the greenhouse air proposed by Meng et al., 2009 can be simplified and differentiated based on eqs (7) and (8), as follows:

$$C_{apth,a} \frac{dT_g}{dt} = \mu A_{si} \left(\frac{dT_{si}}{dt} - \frac{dT_g}{dt} \right) + \mu A_{wn} \left(\frac{dT_{wn}}{dt} - \frac{dT_{gn}}{dt} \right) + \mu A_{we} \left(\frac{dT_{we}}{dt} - \frac{dT_{ge}}{dt} \right) + \mu A_{ww} \left(\frac{dT_{ww}}{dt} - \frac{dT_{gw}}{dt} \right) - \mu_j A_j \left(\frac{dT_g}{dt} - \frac{dT_{out}}{dt} \right) \quad (10)$$

A simplification of [eq. (10)] yields:

$$k = \frac{\mu \times (k_{si} A_{si} + k_{wn} A_{wn} + k_{we} A_{we} + k_{ww} A_{ww}) + \mu_j A_j k_{out}}{C_{apth,a} + \mu_j A_j - (A_{si} + A_{wn} + A_{we} + A_{ww}) \times \mu} \quad (11)$$

From the assumptions in Section 2.1.2 and the study of Hu Jj⁰ of the relationship between indoor and outdoor temperatures, we can simplify [eq. (10)] to give:

$$A = \frac{\mu \times (k_{si}A_{si} + k_{wn}A_{wn} + k_{we}A_{we} + k_{ww}A_{ww})}{C_{apth,a} + \mu_j A_j - (A_{si} + A_{wn} + A_{we} + A_{ww}) \times \mu}$$

$$B = \frac{\mu_j A_j}{C_{apth,a} + \mu_j A_j - (A_{si} + A_{wn} + A_{we} + A_{ww}) \times \mu}$$

We therefore obtain:

$$k = A + Bk_{out} \quad (12)$$

Where:

B is a constant value that is related to the indoor soil area, the area of the east-west and north side walls, and the convective heat transfer coefficient and area of the mulch of the sunken heliostat.

The heat loss from the greenhouse at night can be obtained as follows:

$$Q = \mu_j A_j \left(\frac{Bk - k - A}{B} t + C \right) \quad (13)$$

Where:

$$A = \frac{\mu \times (k_{si}A_{si} + k_{wn}A_{wn} + k_{we}A_{we} + k_{ww}A_{ww})}{C_{apth,a} + \mu_j A_j - (A_{si} + A_{wn} + A_{we} + A_{ww}) \times \mu}$$

$$B = \frac{\mu_j A_j}{C_{apth,a} + \mu_j A_j - (A_{si} + A_{wn} + A_{we} + A_{ww}) \times \mu}$$

From [eq. (13)], we know the following:

(i) The heat released from greenhouse at night is related to time t , the rate of change in the indoor temperature k , and the indoor-outdoor temperature difference C at the moment of closing the shed. The equations for A and B are related to the indoor air heat capacity, the areas of the walls and indoor ground, the heat transfer coefficient between the walls and indoor ground and air, and the heat transfer coefficient and area of maintenance structure. When the area and nature of the wall and the area and nature of the maintenance structure are known, the amount of heat loss in the greenhouse is related to the time and the difference between the indoor and outdoor temperatures at the initial moment, which can provide a theoretical reference for the heating measures.

(ii) The formula for the heat dissipation at night can give the amount of indoor heat loss in the sunken solar greenhouse, and the amount of heat loss is related to the rate of change of indoor air temperature with time. We assume that the temperature drop at each point in the indoor space at night is equal. We therefore need to verify whether the indoor temperatures of sunken solar greenhouse are equal at night. We propose that the basis of heat loss is that the temperature drop at night is equal at each point in the indoor space, meaning that the

calculation of heat loss is simplified and more suitable for practical applications.

Testing instruments

A U-disk temperature recorder includes a precision RC-5 temperature recorder USB automatic data temperature and humidity recorder, and a built-in wide temperature CR2032 battery. The recording interval is six minutes, and it can record continuously for three months; if the built-in battery is regularly replaced, the device can continue to record the temperature. The measuring temperature range for this recorder is -30°C to 70°C ; the accuracy in the range -20°C to 20°C is $\pm 0.5^{\circ}\text{C}$, and in other ranges it is 1°C . The U-disk recorder uses a built-in NTC thermistor, which can store 32,000 sets of data.

Test scheme

It can be seen from [eq. (6)] that the rate of change in the indoor temperature along the transverse direction is the largest, followed by that along the transverse direction, and finally that along the longitudinal direction. Six positions were selected along the horizontal direction of the greenhouse, and seven auxiliary sections were selected in the longitudinal direction in order to conduct multiple cross-sectional

experimental studies on the indoor thermal environment. The test period ran from 26th December 2019 to 2nd June 2020. The temperatures at seven cross sections of the sunken solar greenhouse were measured with a wireless temperature sensor and a U-disk temperature recorder. For each cross section, the intersection between the

indoor ground and the sunken wall surface was taken as point O, the y-axis was horizontally north, and the x-axis was vertically east, establishing the coordinate system shown in Figures 2 and Table 3. A U-disk temperature recorder was installed at an outdoor unshielded height of 1.5 m to record the outdoor temperature value.

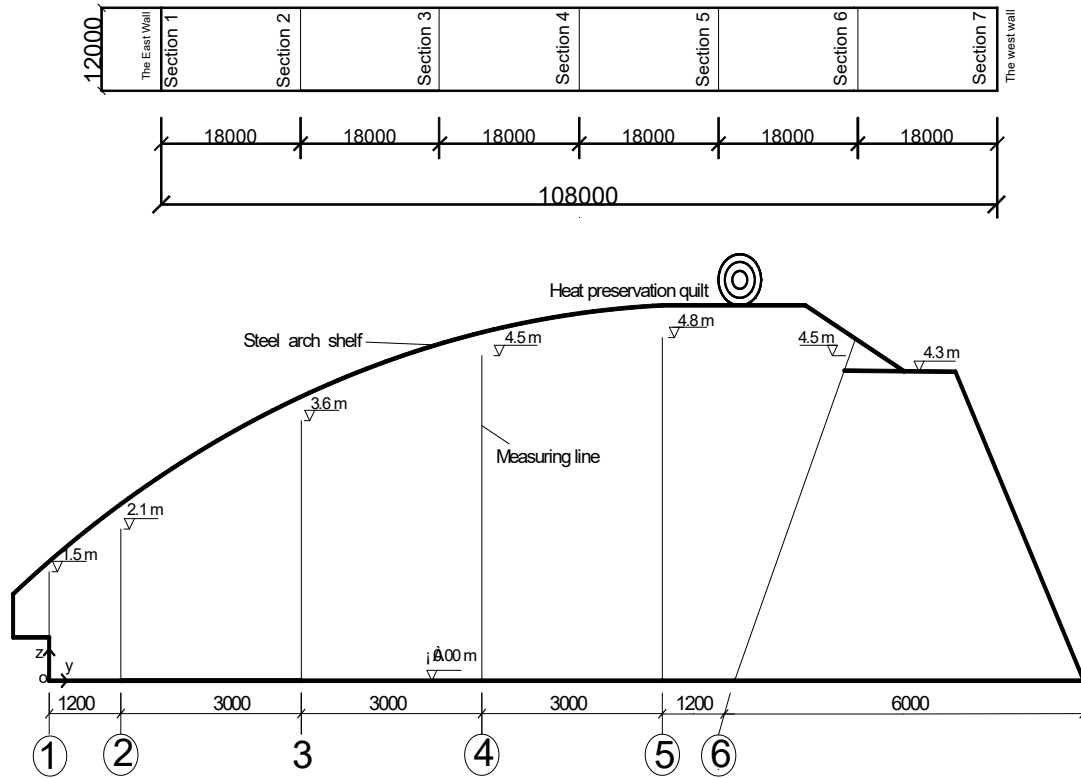


FIGURE 2. Layout of cross section and measuring lines in the greenhouse.

TABLE 3. Heights of measuring points at each cross section.

		Line number					
		1	2	3	4	5	6
y-coordinate		0	1.2	4.2	7.2	10.2	North Wall
Height of measuring point	1	1.5 (+)	2.1 (+)	3.6 (+)	4.5 (+)	4.8 (+)	4.5 (+)
	2	1.2 (-)	1.8 (-)	3.3 (-)	4.2 (-)	4.5 (-)	3.9 (-)
	3	0.9 (-)	1.5 (-)	3 (-)	3.9 (-)	4.2 (-)	3.3 (3)
	4	0.6 (+)	1.2 (+)	2.4 (-)	3.6 (-)	3.6 (-)	2.7 (-)
	5	0.3 (-)	0.6 (-)	1.8 (+)	3 (+)	3 (+)	2.1 (1.8)
	6	0 (+)	0.3 (-)	1.2 (-)	2.4 (-)	2.4 (-)	1.5 (-)
	7	-	0 (+)	0.6 (-)	1.8 (+)	1.8 (+)	0.9 (-)
	8	-	-	0.3 (-)	1.2 (-)	1.2 (-)	0.3 (+)
	9	-	-	0 (+)	0.6 (-)	0.6 (-)	-
	10	-	-	-	0.3 (-)	0.3 (-)	-
	11	-	-	-	0 (+)	0 (+)	-

Legend: (+) means other sections also have this measuring point, (-) means other sections do not have this measuring point, (number) means other sections measuring point height.

RESULTS AND DISCUSSION
Changes in indoor thermal environment

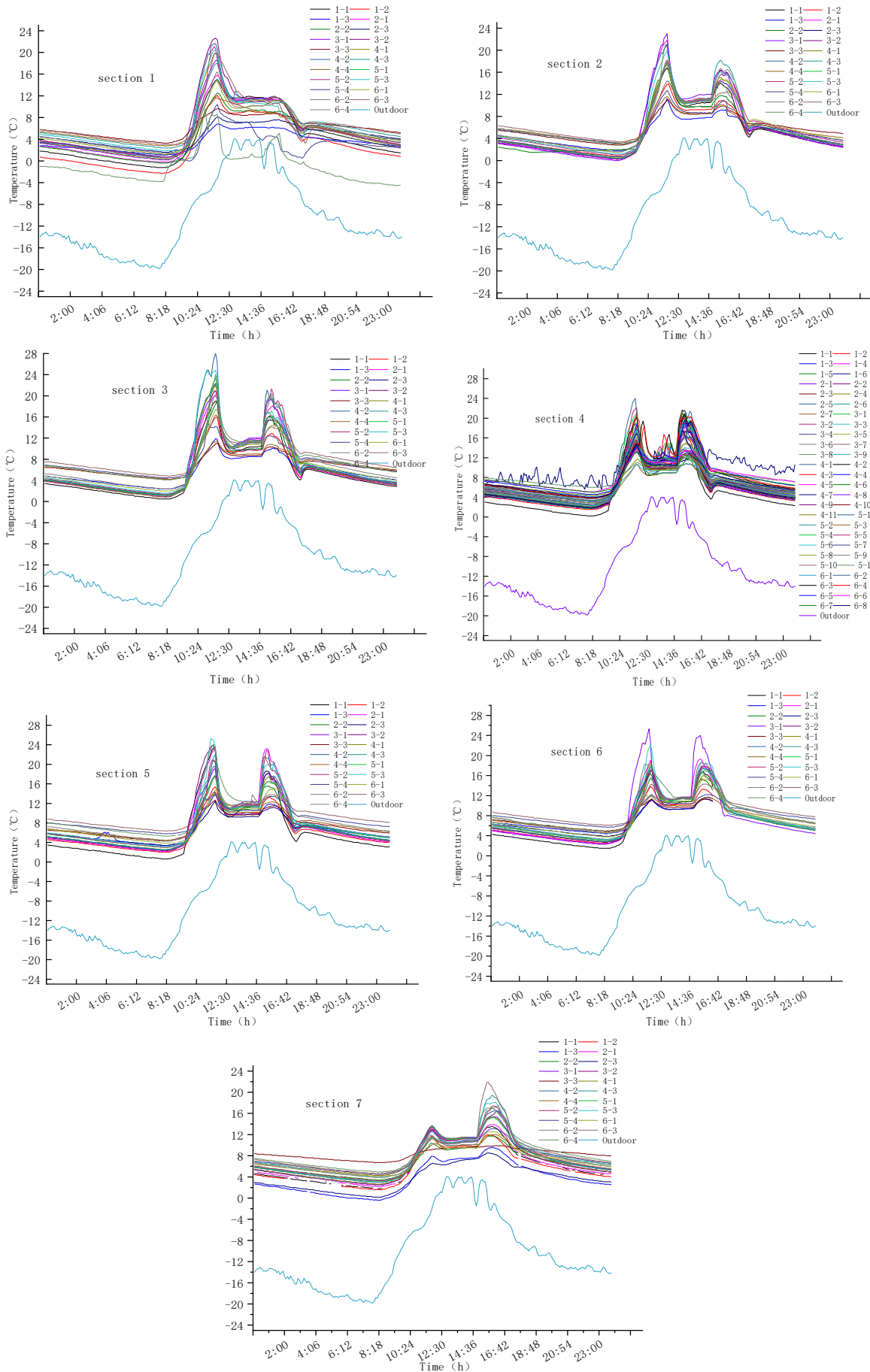


FIGURE 3. Temperature versus time curves for different cross sections (taken on 14th January 2020, sunny and snowy the day before, the coldest day of 2020 in Jinzhong, Shanxi Province)

From the data for the different sections, we see that the temperature at each indoor measuring point at the different sections changes with time. The temperature decreases linearly with time at night (from the closing time to the opening time); the opening time is 12:00, and the temperature of each measuring point then rises with time; between 12:00 and 14:00 fluctuation rise; 13:00 is the closing time, and the temperature at each measuring point decreases with time.

TABLE 4. Minimum temperature values at different cross sections, on 14th January 2020 (°C).

Line number	Height from indoor floor (m)	Cross section						
		1	2	3	4	5	6	7
1	0	1.2	1.8	2.4	3.2	3.4	4.5	–
	0.6	–2.3	0.8	1	1.9	2	2.5	1.6
	1.5	–1.2	0.3	0.5	0.2	0.6	1.5	1.9
2	0	1.7	–	–	2.8	3.4	4	4.2
	1.2	–0.4	0	1.3	2.2	2.5	2.8	3.5
	2.1	–0.2	0.3	0.9	2	2.2	2.4	2.2
3	0	3.4	2.9	4.3	4.2	4.3	5	6.8
	1.8	0.7	0.4	1.2	2	2.3	2.8	2.6
	3.6	0.2	0	1	1.7	2.5	2.3	2.6
4	0	2.8	3.2	4.2	6	4.5	4.7	4.3
	1.8	2.4	1	1.3	2.6	2.5	3.1	3
	3	0.6	0.7	1.2	2.3	2.5	2.9	3
	4.5	0.4	0.5	0.9	2.3	2.5	2.9	2.7
5	0	2	–	4.5	6	5.8	5.8	4.6
	1.8	1	–	1.6	2.6	3.2	3.3	4
	3	0.7	1.1	1.4	2.3	3.1	3.3	3.3
	4.8	–	–	1.2	2.3	3	3.2	3.2
6	0.3	3.8	2.9	4.1	4	5.3	4.9	5
	1.8	3.1	3.4	4.9	–	6.4	6.2	4.7
	3	1.5	1.6	2.4	–	4.4	4.6	4
	4.5	1.3	1.5	2	3.1	3.9	3.9	4.2

On the night of 14th January 2020, 86% of the indoor measurement points had a minimum value of temperature below 5°C. Line 5 of each cross-section represents the planting end, and the measurement point for line 5 showed the highest value of nighttime air temperature for each cross-section of the planting area at the same height. However, the temperature values at each measurement point for line 5 were lower than 5°C for about five hours, meaning that when the outdoor temperature is low, heating measures should be applied to the sunken solar greenhouse.

The minimum values of the indoor air temperature in the sunken solar greenhouse varied horizontally, vertically, and vertically, a finding that is aligned with those of Xu (2018) and Zhang et al. (2019), among others. However, these researchers did not study the rate of change in the indoor nighttime low temperatures in three-dimensional coordinates or the length of the low-temperature period.

Rate of change of indoor 3D thermal environment in winter

Cross-section 4 was in the middle of the sunken daylight greenhouse, cross-section 1 was at the east wall, and cross-section 7 was at the west wall. The minimum value of the indoor temperature at 86% of the measured points was less than 5°C, an unfavourable temperature for the growth and development of strawberries. The minimum value of the indoor air temperature for the sunken heliostat differed in the horizontal, vertical and vertical directions, and the rates of change in the indoor low temperature at night were different in each of the three-dimensional directions.

7 cross-sections, different cross-sections with the same height and the same horizontal position of the maximum temperature difference at night is 4.8°C, for cross-section 1 0.6 m at the measuring point and cross-section 6 0.6 m at the measuring point. At this time, the minimum value of the indoor temperature at night

along the longitudinal maximum temperature change rate of $0.053^{\circ}\text{C}/\text{m}$. The maximum temperature difference between the measurement points for the same cross-section and the same height was 2.8°C , which was the measurement point at 0 m of measurement line 1 in cross-section 4 and the measurement point at 0 m of measurement line 4 for cross-section 4. The rate of change in the maximum temperature difference along the horizontal direction was $0.38^{\circ}\text{C}/\text{m}$. The maximum temperature difference between the measurement points in the same cross-section and the same measurement line was 4.2°C , which was the temperature difference between the measurement point at 0 m of measurement line 3 in cross-section 7 and the measurement point at 3.6 m of measurement line 3 in cross-section 7.

The rate of change in the indoor temperature minimum at night along the vertical maximum temperature difference was $1.17^{\circ}\text{C}/\text{m}$. The rate of change in the maximum temperature difference along the height direction in the greenhouse was found to be 13 times that along the vertical direction, and three times that along the horizontal direction.

From an analysis of the maximum indoor temperature, we see that the rate of change of the maximum temperature difference along the vertical height is 13.4 times that along the vertical direction, and 7.2 times that along the horizontal direction.

Comparative analysis of the daytime heat-absorption model and experimental data

From Section 3.1.1, it can be seen that order of the rates of change in the maximum indoor temperature of the sunken solar greenhouse, from large to small, is as follows: rate of change along the vertical direction > rate of change along the horizontal direction > rate of change along the longitudinal direction. The experimental results presented above are consistent with the theoretical expression in [eq. (7)]: the rate of change in the indoor temperature in the solar greenhouse is greatest along the vertical direction, followed by the horizontal direction, and finally the longitudinal direction. Hence, it is important to study the law governing the change in the indoor temperature along the vertical direction.

Comparison of night-time indoor temperature changes with the nighttime heat-dissipation model

The ranges of the temperature drops at all measurement points in all cross-sections during the time period 0:00 to 8:00 are $-2.7\pm 0.4^{\circ}\text{C}$, $-2.7\pm 0.4^{\circ}\text{C}$, $-2.6\pm 0.4^{\circ}\text{C}$, $-2.5\pm 0.2^{\circ}\text{C}$, $-2.6\pm 0.3^{\circ}\text{C}$, $-2.6\pm 0.4^{\circ}\text{C}$, and $-2.8\pm 0.3^{\circ}\text{C}$. The differences in the temperature drops at each measurement point at each cross-section are less than or equal to 0.8°C , and the accuracy of the equipment is $\pm 0.5^{\circ}\text{C}$, meaning that the drops in temperature at each measurement point in this time period are approximately equal. This verifies the correctness of the nighttime heat-dissipation model presented in Section 1.1.2; i.e., the rates of change in the indoor space point temperatures at night are the same throughout the sunken solar greenhouse.

Relationship between indoor and outdoor temperature changes

Hourly mean temperature values were obtained for the time period 0:00 to 8:00 at each measurement point along cross-section 4 on 14th January 2020, giving a total of eight sets of data for each measurement point. A coordinate system was established with the southwest bottom of the greenhouse interior as the origin, the positive x -axis towards the east, the positive y -axis towards the north, and the upward vertical direction as the positive z -axis. This coordinate system was established to fully consider the low temperature area on the east side and ignore the higher temperature soil wall on the west side, and to neglect the temperature value at measurement point 6 for each section, as this was the temperature at the inner surface of the wall on the north side, at the intersection between the air and soil.

Considering the distribution of the indoor temperatures in the horizontal, vertical and longitudinal directions of the sunken solar greenhouse, a weighted value of the indoor temperature was derived using the formula:

$$\bar{t} = \frac{\sum x_i y_i z_i t_i}{\sum x_i y_i z_i} \quad (11)$$

Using [eq. (12)], the hourly average weighted indoor temperatures of the sunken solar greenhouse during the time period 0:00 to 8:00 were calculated as 3.8°C , 3.5°C , 3.2°C , 2.8°C , 2.5°C , 2.1°C , 1.8°C , and 1.6°C . The hourly average outdoor temperatures during this period were -13.6°C , -13.7°C , -15.3°C , -16°C , -17.8°C , -18.5°C , -19°C , and -19.5°C . Using the outdoor temperature as the x -axis and indoor temperature as the y -axis, a scatter plot was drawn to represent the data, which were fitted with an R^2 greater than 0.95 (i.e., a good fit).

The equation relating the indoor-outdoor temperatures was found to be $y = 0.3456x + 8.4325$, where y is the indoor temperature ($^{\circ}\text{C}$), and x is the outdoor temperature ($^{\circ}\text{C}$). From this equation, we can see that at night in winter, when the sunken greenhouse is covered with polyethylene multifunctional composite film and an acrylic cotton insulation quilt is placed on the south side of the roof, the indoor temperature is linearly related to the outdoor temperature value, and the indoor temperature decreases by 0.35°C for every 1°C drop in outdoor temperature.

Time period and marginal effect determination methods

From the results presented in Section 3.3, we see that (i) the temperatures at different heights along the same measurement line are different; (ii) there are measurement points with equal night-time temperatures close to the membrane; and (iii) the vertical region between measurement points with approximately equal temperatures is most affected by the outdoor temperature, as the air temperatures in this region are approximately equal and heat conduction with the outdoor air occurs through the membrane.

Determination of time periods: We used the data processing method described by Sun Zhiqiang⁰, and divided the indoor temperature of the sunken solar greenhouse during winter into four time periods, representing four conditions: rising, falling, extreme values, and minimal values. Each day was divided into periods 00:00 to 08:00 (including 8:00 data), 08:00 to 13:00 (excluding 8:00 data, including 13:00 data), 13:00 to 18:00 (excluding 13:00 data, including 18:00 data), and 18:00 to 24:00 (excluding 18:00 data). These four time periods were used to find the average temperature at each measurement point over each time period. Using the height of each measurement line as the horizontal coordinate and the average temperature of the measurement points in the corresponding time period as the vertical coordinate, a scatter plot was drawn.

The method used to determine the marginal effect curve under the trellis membrane was as follows: the average temperature at measurement point 1 of each measurement line was used as a control value for the average temperature at each measurement point of the same measurement line (not counted in the scatter plot). The measurement points near the ground (where the height of the upper surface of the indoor floor was 0 m) are not included in the chart.

The method of determining the marginal effect curve at the ground was as follows: the mean value of the temperature at the measurement point 0.3 m above the indoor ground surface for each measurement line was taken as the control value (not included in the scatter diagram); the measurement point near the ground (and 0

m above the indoor ground surface) was also not included in the curve. Scatter plots were created of the mean temperature values at the measurement points in the marginal effect under the trellis membrane and the marginal effect on the ground in relation to the height of the measurement points, and the data were fitted to obtain the curve equations.

The boundary point of the marginal effect method was determined as follows: the average temperature at measurement point 1 of each measurement line and the average value of the temperature of measurement point at 0.3 m as T value, respectively, brought into the corresponding measurement line of the marginal effect curve under the scaffolding film and the equation of the marginal effect curve on the ground, respectively, to calculate the respective z value, the determined z value for the boundary point of the marginal effect under the scaffolding membrane and the boundary point of the marginal effect on the ground, respectively.

Since the sunken solar greenhouse was mainly designed to improve the thermal environment of the plants at night, the marginal effect was studied over the time period 0:00 to 8:00. The temperatures at each measurement point during this time period were averaged, and the method of determining the equations for the marginal effect curves under the shed membrane and on the ground was used to determine the equation for the marginal effect curve.

Marginal effect analysis for the period 0.00 to 08.00

TABLE 5. Marginal effect curves for indoor air temperature for the period 0:00 to 8:00 on 14th January 2020.

Line no.	Marginal curve position	Fitting function
1	Marginal effect curve equation for trellis	$T = 0.9433z^2 - 2.3626z + 4.2601$
	Equation for soil marginal effect curve	$T = -1.1204z^2 + 1.3672z + 2.6863$
2	Marginal effect curve equation for trellis	$T = -0.0629z^2 - 0.0024z + 3.3119$
	Equation for soil marginal effect curve	$T = 0.0241z^2 - 0.2049z + 3.4151$
3	Marginal effect curve equation for trellis	$T = -0.0593z^3 + 0.5192z^2 - 1.5135z + 4.6135$
	Equation for soil marginal effect curve	$T = -0.1983z^3 + 1.4328z^2 - 3.3233z + 5.6388$
4	Marginal effect curve equation for trellis	$T = -0.0909z^3 + 0.7953z^2 - 2.2195z + 5.1864$
	Equation for soil marginal effect curve	$T = -0.0977z^3 + 0.8856z^2 - 2.528z + 5.4603$
5	Marginal effect curve equation for trellis	$T = 0.136z^2 - 1.02z + 5.409$
	Equation for soil marginal effect curve	$T = 0.1465z^2 - 1.0935z + 5.5179$
6	Marginal effect curve equation for trellis	$T = -0.1026z^2 - 0.0728z + 6.4288$
	Equation for soil marginal effect curve	$T = -0.0057z^2 - 0.5449z + 6.9252$

As shown in Table 5, the correlation coefficient of the curve equation $R^2 > 0.9$, and the boundary curve equation of each measurement line was well fitted.

The temperature at measurement point 1 of each measuring line was substituted into the equation of the marginal effect curve under the membrane as the T value, and the corresponding z value was derived, which was judged to be the boundary point of the marginal effect under the membrane for that measuring line. The results

show that the difference between the lowest temperature at the first measuring point near the membrane and the average temperature for the measuring line in the same time period was less than 0.5°C during the night of 14th January 2020. The mean temperature on the measuring line in the time period 0:00 to 8:00 was put into the curve equation for the marginal effect under the membrane, and the vertical height corresponding to the mean temperature for the measuring line was obtained. The

temperature difference between this height and the area formed by the boundary point of the marginal effect under the shed film was less than 0.5°C.

The temperature at the measuring point 0.3 m from the ground for each measuring line was substituted into the equation for the boundary point of the marginal effect on the ground of the corresponding measuring line as the T value, and the z value was determined, which was considered the boundary point for the marginal effect at the ground for the measuring line. In order to study the relationship between the boundary point of the

marginal effect and the horizontal distance in a more intuitive way, a scatter plot was drawn of the length of the line, the boundary point of the marginal effect, the mean height of the temperature of the line, and the horizontal distance between the line and the sunken wall. We assumed that the y -coordinate for measurement line 6 was 11.5 m (representing the horizontal distance between the bottom of the north wall of the sunken heliostat and measuring line 1; the interior of the north wall was tilted from the interior to the outside).

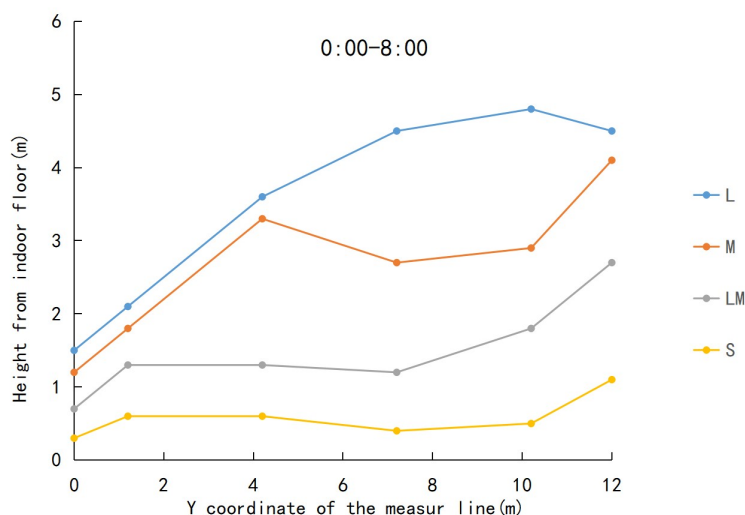


FIGURE 4. Relationships between boundary points of marginal effect and horizontal position during the period 0:00–8:00 on 14th January 2019.

In Figure 4, L represents the length of the measurement line, M represents the boundary point of the marginal effect under the greenhouse membrane, S represents the boundary point of the marginal effect on the ground, and LM represents the vertical height corresponding to the mean temperature value of the measurement line.

It can be seen from Figure 5 that with an increase in the y coordinate value of the measuring line, the boundary point of the marginal effect under the greenhouse membrane gradually rose. For measuring line 4, located to the centre and to the north of the greenhouse, the area of the marginal effect under the greenhouse film reached 1.8 m, the vertical height difference between the length of the measuring line and the mean value of the measuring line temperature was 3.3 m, the temperature difference between the measuring points in this area was less than 0.5°C, and the low temperature area range was larger at this time. With an increase in y , the mean value of the measuring line temperature vertical height gradually increased: the vertical height of the measuring line mean temperature within the indoor planting area was less than 2 m; the area affected by the marginal effect under the greenhouse membrane was larger in the middle of the greenhouse, and the area affected by the marginal effect under the greenhouse membrane on the south and north sides of the greenhouse became smaller. The greenhouse soil boundary point was more stable, and fluctuated at a height of about 0.6 m from the indoor

ground. The vertical height of the average measured line temperature increased with y , and the mean temperature of each measuring line increased under the extreme conditions at night. At night, the difference between the temperature value of the vertical height point of the mean temperature value of each measuring line and the temperature of the boundary point of the marginal effect under the greenhouse membrane was less than 0.5°C, and the difference between the temperature of the vertical height point of the mean temperature value of each measuring line and the temperature value of the boundary point of the marginal effect on the ground was less than 1.1°C. Determining the boundary point of the marginal effect under the trellis membrane and the height of the mean temperature value for the measuring line can provide theoretical data for the height of stereoscopic planting and the heating area at night, meaning that frost damage to indoor plants can be avoided in extreme climates.

Marginal effects under the trellis membrane during the time period 0:00 to 8:00 in different months

We considered the data for the measuring points at the span-centre position of the middle cross-section of the greenhouse during the time period of 0:00–8:00 from January to March 2020. The temperature values at each measuring point were averaged over 1 h, giving a total of eight data samples for each measuring point, and the temperature at each measuring point was analysed for

significance with the temperature values of the first measuring point of the same measuring line at 5% significance level, using a single-factor Duncan multiple comparison and an ANOVA in SPSS software. Based on the definition of the boundary point of the marginal effect

under the trellis membrane given in Section 3.3.1, the boundary point for the marginal effect under the trellis membrane was derived, and a scatter plot of the boundary point of the marginal effect under the trellis membrane versus time was plotted as shown in Figure 6.

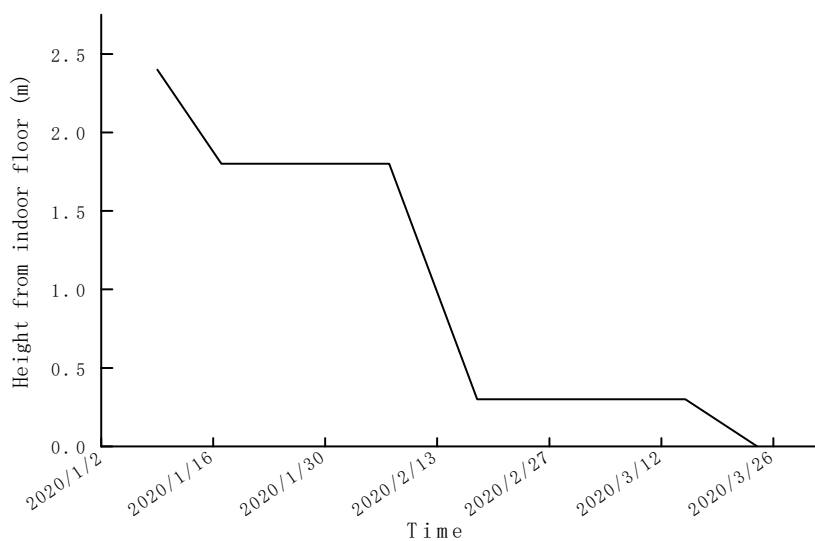


FIGURE 5. Boundary points for the membrane boundary effect in the middle of greenhouse in different months.

From the software analysis, we find that the boundary point of the marginal effect under the greenhouse film at measuring line 4 across the middle of the greenhouse cross-section is measuring point 8, which is 1.2 m away from the indoor height, and this height is the vertical height point corresponding to the mean value of the measuring line temperature, because the temperature difference between the vertical height point of the mean value of the measuring line temperature in the middle of the greenhouse and the vertical boundary point of the greenhouse film is less than 0.5°C at night.

From Figure 5, we see that the boundary point of the marginal effect under the greenhouse film at the cross-sectional position of the greenhouse remains unchanged over a certain time period, and the height of the marginal effect under the greenhouse membrane at the cross-sectional position of the greenhouse in early January is 2.5 m. The area of the marginal effect under the greenhouse membrane is equal to the roof height at this horizontal position minus the boundary point of the marginal effect under the greenhouse membrane, and the height of the greenhouse membrane from the indoor floor here is 4.5 m. Hence, from mid-January to early February, the height of the boundary point of the marginal effect under the greenhouse film at the cross-sectional position remains unchanged at about 1.8 m from the indoor floor, and the area of influence of the marginal effect under the greenhouse film reaches 2.7 m. From mid-February to mid-March, its position about 0.3 m from the indoor floor. From mid-February to mid-March, this boundary point is located at about 0.3 m from the indoor floor, and the temperature of the measured point at 0.3 m from the floor is less than 0.4°C compared with that at 4.5 m, so the temperature difference in this area can be considered small.

The marginal effect of the temperature environment of solar greenhouses is very clear, and the temperature environment of the marginal area of solar greenhouses has been discussed in the literature by many researchers (Chen, 2005). However, few studies have been conducted on the marginal effect under the canopy, and our results can therefore provide a good reference basis for solar greenhouse heating and cold protection.

CONCLUSIONS

In this paper, we have explored the three-dimensional thermal environment and marginal effects of a sunken solar greenhouse; based on previous theoretical research, we have derived a formula for the heat absorption of indoor air in a solar greenhouse by applying the principles of architecture and thermodynamics, proposed a theoretical equation for heat absorption of indoor air with horizontal and vertical coordinates, and explained the changes in the indoor temperature in the horizontal, vertical and longitudinal directions. Based on the theory of internal heat dissipation in the greenhouse, the relationship between indoor heat dissipation and the rate of change in the outdoor temperature was established to provide theoretical guidance for greenhouse heating in winter. A multi-cross-sectional temperature test was conducted to explore the variation in the indoor temperature along the longitudinal, lateral and vertical directions of the greenhouse, to verify the theoretical model, and to explore the marginal effect area based on air temperature. The main conclusions of our work are as follows:

(i) The correlation between the heat absorption at the indoor space point and the vertical position z of the point

was the greatest, followed by the horizontal position y , and finally the vertical position x .

(ii) Experimental data verified the correctness of the theoretical models; that is, the maximum rate of change in the temperature along the vertical direction and the decline in the values at each measurement point at night were approximately equal.

(iii) When the sunken solar greenhouse was covered with a polyethylene multifunctional composite membrane and an acrylic cotton insulation quilt on the south side of the roof, the indoor temperature was linearly correlated with the outdoor temperature, and decreased by 0.35°C for every 1°C drop in outdoor temperature. Different values of thermal resistance will be produced for different greenhouse membranes and warming quilts. Changes in thermal resistance values will affect the degree of temperature loss inside the greenhouse.

(iv) The area of marginal effect under the greenhouse membrane varied with the time and month. In January 2020, the minimum area of marginal effect was 2 m, and the maximum area was 2.7 m at the mid-span position of the greenhouse mid-section.

ACKNOWLEDGMENTS

The author is grateful for support from the Shanxi Agricultural University Outstanding Doctoral Initiation Program (2023BQ06).

REFERENCES

- Ahamed Md S, Guo H, Tanino K (2018) Sensitivity analysis of CSGHEAT model for estimation of heating consumption in a Chinese-style solar greenhouse. *Computers and Electronics in Agriculture* 154:99-111. <https://doi.org/10.1016/j.compag.2018.08.040>
- Bao EC, Cao YF, Zou ZR, Zhang Y (2019) Heat transfer characteristics of solar greenhouses with different structures of active thermal storage walls. *Journal of Agricultural Engineering* 35(3):189-197. <https://doi:10.11975/j.issn.1002-6819.2019.03.024>
- Chen DS (2005) Microclimate environment and its regulation in solar greenhouse. *China Flower Horticulture* (8):47-52. CNKI:SUN:HYZG.0.2005-08-00M
- Guan Y, Chen C, Li Z, Han YQ, Ling HS (2012) Improvement of thermal environment of solar greenhouse by phase change material wall. *Journal of Agricultural Engineering* 28(10):194-201. CNKI:SUN:ZGSC.0.2012-18-020
- Han YD, Xue XW, Luo XL (2014) Construction of solar radiation estimation model in solar greenhouse. *Journal of Agricultural Engineering* 30(10):174-181. <https://doi.org/10.3969/j.issn.1002-6819.2014.10.022>
- Hu JJ, Fan GS (2018) Heat transfer characteristics of soil and air in overwintering heliographic greenhouses. *Soil Bulletin* 49(4): 869-875. CNKI:SUN:TRTB.0.2018-04-016.
- Hu JJ, Fan GS, Gao YJ (2014) Experimental study on the characteristics of air temperature change in overwintering heliotope. *Journal of Taiyuan University of Technology* 45(4):490-495. <https://doi.org/10.3969/j.issn.1007-9432.2014.04.013>
- Huang X, Wang XF, Wei M, Hou JL, Liu FS, Li QM, Yang FJ, Shi QH (2013) Variation patterns of temperature and heat flow in the soil wall of undercut heliotope greenhouse. *Journal of Applied Ecology* 24(6):1669-1676. CNKI:SUN:YYSB.0.2013-06-029
- Liu BYH, Jordan RC (1960) The relationship and characteristics distribution of direct diffuse and total radiation. *Solar Energy* 4(3):1-19. [https://doi.org/10.1016/0038-092X\(60\)90062-1](https://doi.org/10.1016/0038-092X(60)90062-1)
- Ma CW, Zhao SM, Cheng JY, Wang N, Jiang YS, Wang SY, Li BM (2013) Study on the construction of a model of solar greenhouse light radiation environment. *Journal of Shenyang Agricultural University* 44(5):513-517. <https://doi:10.3969/j.issn.1000-1700.2013.05.001>
- Ma YH, Li BM, Wang GQ, Liu N, Liu D (2019) Temperature increase and strawberry cultivation effect of assembled solar greenhouse masonry with different heat storage walls. *Journal of Agricultural Engineering* 35(15):175-181. CNKI:SUN:NYGU.0.2019-15-022
- Meng LL, Yang QC, Gerard P.A. Bot, Wang N. (2009) Construction of a thermal environment simulation model for daylight greenhouses. *Journal of Agricultural Engineering* 25(1): 164-170. CNKI:SUN:NYGU.0.2009-01-038.
- Ntinis GK, Koukounaras A (2015) Effect of energy saving solar sleeves on characteristics of hydroponic tomatoes grown in a greenhouse. *Scientia Horticulturae* 194:126-133. <https://doi.org/10.1016/j.scienta.2015.08.013>
- Tong G, Christopher DM, Li B (2019) Numerical modeling of temperature variations in a Chinese solar greenhouse. *Computers and Electronics in Agriculture* 68(1):129-139. <https://doi.org/10.1016/j.compag.2009.05.004>
- Tong GH, Christopher DM (2019) Study on the temperature variation law of heat storage and exothermic layer of solar greenhouse wall. *Journal of Agricultural Engineering* 35(7):170-177. CNKI:SUN:NYGU.0.2019-07-021.
- Xu HJ, Cao YF, Li YR, Gao J, Jiang WJ, Zou ZR (2019) Construction and application of solar radiation model for daylight greenhouse. *Journal of Agricultural Engineering* 35(7):160-169. <https://doi:10.11975/j.issn.1002-6819.2019.07.020>

Xu HJ, Li YR, Cui YM, Jiang WJ, Zou ZR (2018) Thermal performance test and analysis of solar greenhouse in hinterland of Hetian desert, Xinjiang. Transactions of the Chinese Society of Agricultural Engineering 34(Supp.): 60-65.
<https://doi.org/10.11975/j.issn.1002-6819.2018.z.010>

Yu MH, Gao GL, Ding GD (2015) A review of plant body temperature studies. Journal of Ecology 34(12):3533-3541. CNKI:SUN:STXZ.0.2015-12-036

Zhang CK, Wei M, Liu FS, Xu L, Li Y (2019) Non-stationary thermal conductivity process of soil at night in a down-digging daylight greenhouse. Journal of China Agricultural University 24(1):108-118.
<https://doi.org/10.11841/j.issn.1007-4333.2019.01.15>

Zhang JH, Shen KC, Chen DY, Zhang MK, Zhang HH, Hu J (2021) Analysis of spatial and temporal variation patterns of canopy characteristic temperature in heliostat based on Internet of Things. Journal of Agricultural Machinery 52(7):336-342.
<https://doi.org/10.6041/j.issn.1000-1298.2021.07.036>

Zhang LH, Zhang F, Liu S, Xu L (2010) Three-dimensional non-stationary simulation of indoor temperature field in a sunken earth-walled greenhouse. Journal of Solar Energy 31(8):965-971.
CNKI:SUN:TYLX.0.2010-08-010.

Zhang QW, Jia Y, Li C, Cui NB, Feng Y, Gong DZ, Hu XT (2018) Evaluation of the applicability of daily radiation model based on meteorological data in northwest China. Journal of Agricultural Engineering 34(2):189-196.
<https://doi.org/10.11975/j.issn.1002-6819.2018.02.026>

Zhang ZL (2012) Research on the heat transfer characteristics of sunken solar greenhouse soil walls. Henan, College of Horticulture, Henan Agricultural University. <https://doi.org/10.7666/d.y2157301>

Zhang ZL, Wang SQ, Liu ZH, Sun ZQ (2012) Experiment and analysis of thermal characteristics of sunken solar greenhouse soil walls. Journal of Agricultural Engineering 28(12):208-215.
<https://doi.org/10.3969/j.issn.1002-6819.2012.12.034>